

## Electrodeposition of 3D microstructures on silicon

This content has been downloaded from IOPscience. Please scroll down to see the full text.

1993 J. Micromech. Microeng. 3 123

(<http://iopscience.iop.org/0960-1317/3/3/007>)

View [the table of contents for this issue](#), or go to the [journal homepage](#) for more

Download details:

IP Address: 129.21.35.191

This content was downloaded on 16/02/2015 at 23:37

Please note that [terms and conditions apply](#).

# Electrodeposition of 3D microstructures on silicon

J Gobet, F Cardot, J Bergqvist and F Rudolf

CSEM Swiss Center for Electronics and Microtechnology Inc, Maladière 71, CH-2007 Neuchâtel, Switzerland

**Abstract.** Metal electrodeposition combined with resist micropatterning techniques provides a powerful tool for the fabrication of thick metallic microstructures. This paper discusses the main characteristics of the electrodeposition process and describes the specific properties of negative polyimide and positive photoresists. The innovative use of this technique is illustrated by the presentation of two realizations, an on-chip high-density array of electromagnets developed for high-performance printing heads, and a micromachined microphone. These realizations demonstrate not only that real 3D electroplated microstructures are achievable but also that integration of electronics is possible on the same silicon substrate.

## 1. Introduction

Metal electrodeposition combined with resist micropatterning techniques provides a powerful tool for the fabrication of thick metallic microstructures. The principle is the selective electrodeposition of a metal on a conductive seed layer through openings in an insulating mask. This deposition technique is characterized by a very high conformity to the mask and the possibility of achieving high aspect ratios. It covers a wide range of applications such as in the fabrication of thin-film recording heads [1], x-ray masks [2, 3], and microelectronic circuit bumps for tape automated bonding (TAB) [4, 5]. Presently, this technique is successfully applied to the fabrication of microelectromechanical sensors and actuators [6–14].

Photosensitive polymers are the most utilized mask materials. They are patterned by UV light, e-beam or x-ray radiations. Dry etching is used for patterning non-photosensitive polymers. This paper will report on microphotolithography, which is widely available in microelectronic laboratories. The x-ray exposure technique at the origin of the well known LIGA process [15, 16], requires a synchrotron source and will not be considered here. It will only be mentioned that this technique can achieve extremely high aspect ratios, up to 100, for thicknesses of 300  $\mu\text{m}$  and more.

A large number of metals and metal alloys are electrodeposited in conventional electrodeposition processes. The fabrication of microstructures however relies mainly upon nickel, iron–nickel, gold and copper. Successful processes have to meet a number of specific requirements. These include a suitable seed layer, a compatible photoresist and the control of the deposit properties such as thickness uniformity, morphology and physical characteristics.

The innovative use of this electrodeposition technique is emphasized in this paper by presenting two CSEM realizations, an on-chip high-density array of electromagnets for high-performance magnetographic printing heads, and a micromachined microphone. These realizations furthermore demonstrate that the electrodeposition technique is compatible with silicon micromachining as well as with the integration of associated electronics.

## 2. Photoresist processes

The geometrical features of the microdevices depend on the performance of the photoresist material and that of the patterning technique. The processes involved, such as spin coating, alignment, exposure and development, are basically the same as those employed in standard microelectronic technology. However, they have to be adapted in order to meet a number of specific challenges when fabricating microstructures. Thicknesses of a few micrometers up to 50  $\mu\text{m}$  or more are required, together with precise demands on wall characteristics. In addition, the photoresist has to withstand the electroplating bath without being damaged. To achieve these goals, both negative and positive photoresists are being used in fabrication processes.

### 2.1. Negative photoresists

Photosensitive polyimide precursors are frequently employed for realizing microstructures in the thickness range of 10–50  $\mu\text{m}$  [17, 6–9, 12]. The fabrication process follows broadly that used for gold bumps in microelectronics [5]. It results in patterns characterized by straight, almost vertical walls with angles of 89°

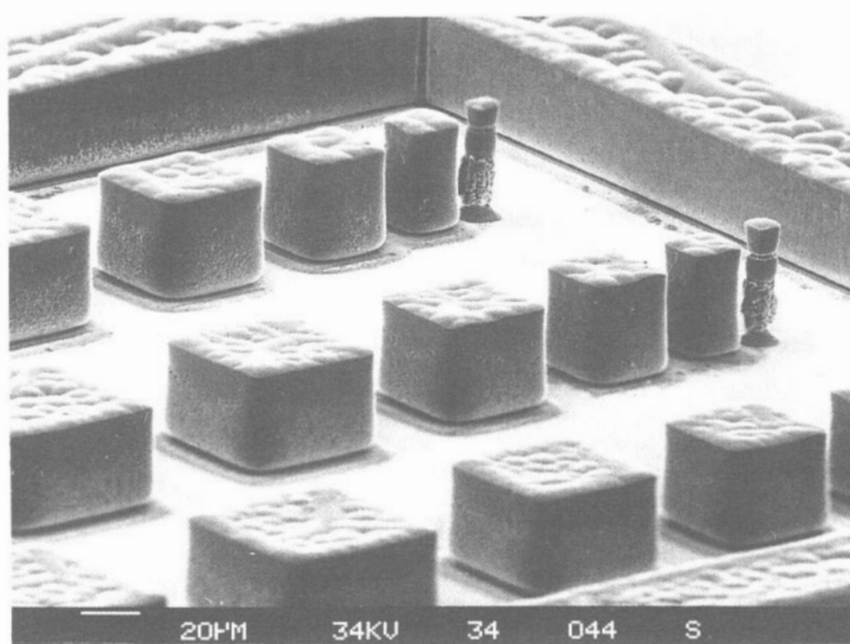


**Figure 1.** Electrodeposited FeNi test structures after stripping the Probimide mold. The structures are 40  $\mu\text{m}$  high and 10–50  $\mu\text{m}$  on each side.

and aspect ratios larger than two on flat surfaces. Aspect ratios as high as eight have been reported but with a strong dependence on layout geometries [17]. After prebake, exposure and development, the polyimide precursor layer shows adequate mechanical properties as well as a good stability towards slightly basic or acid plating solutions at bath temperatures of around 50 °C. To transform the esterified polyamic acid precursor into a stable polyimide film that can be retained as a dielectric layer in the product, a thermal treatment at 400 °C under nitrogen is needed. This step however reduces the original layer thickness by almost 40%. Figure 1 presents, as an example, FeNi test structures realized with OCG Probimide 348. The Probimide was spun for 10 s at 500 RPM and 30 s at 1000 RPM, prebaked for 30 min at 115 °C on a hot plate, exposed under vacuum contact and developed. After FeNi electrodeposition, the Probimide was stripped in XB-4234 at 80 °C. The 40  $\mu\text{m}$  high structures show that aspect ratios as high as four can be achieved although the walls may be somewhat irregular. The shape of the pole feet indicates that the Probimide has been partially polymerized by light scattered at the metallic interface and therefore not fully developed. This scattered light and the light reflected in non-uniform interfaces give rise to one important restrictive effect when patterning small openings in negative photoresists, because this results in insoluble crosslinked intermediates.

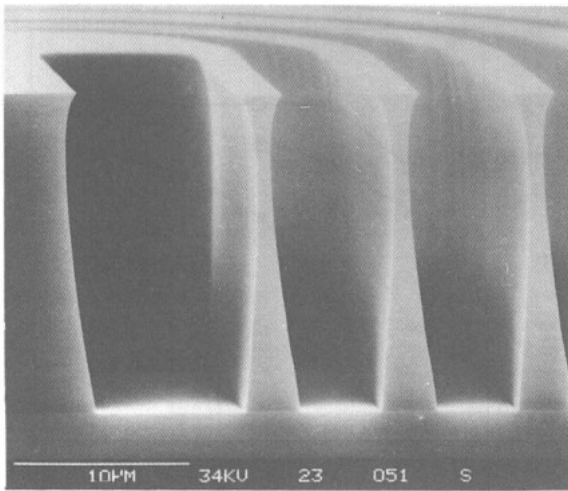
Difficulties encountered when stripping the polyimide after electrodeposition may also restrict its use. The organic-base stripper acts indeed by swelling the uncured resist without completely dissolving it. In some cases, this effect can prevent the full elimination of the polymer mask.

## 2.2. Positive photoresists

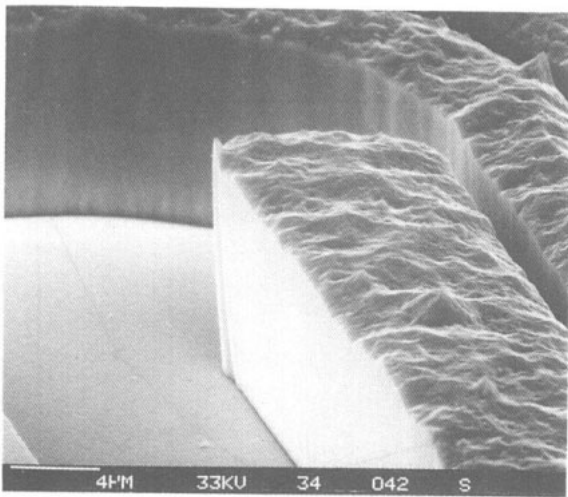
Thick positive photoresists are commercially available in thickness ranges of 2–10  $\mu\text{m}$  (AZ4500 from Hoechst), or up to 20  $\mu\text{m}$  (STR1000 from Shipley). Thicker layers, up to 80  $\mu\text{m}$ , have been achieved by multiple coatings, each layer being baked before applying the next one [18, 19]. Positive resists allowing the realization of 40  $\mu\text{m}$  layers in one coat are being developed or are in a precommercial phase. These products are characterized by a high viscosity and a high transparency. Positive photoresists are normally used in standard microelectronic processes. They achieve high resolutions and aspect ratios, typically three and up to seven according to the literature [18]. They are easy to strip. Figure 2 presents a polymer mold realized in thick STR1110 positive photoresist. This resist, applied in a single coat, was spun for 30 s at 2000 RPM, prebaked for 30 min at 90 °C in an oven, exposed under vacuum contact and developed in Microposit 322 alkaline developer. The 17  $\mu\text{m}$  high structures are realized with a mask linewidth of 3.2  $\mu\text{m}$  and a pitch of 8  $\mu\text{m}$ . The cross-section shows typical profiles of the mold cavities. With positive resists, the exposure energy used to develop the grooves has produced enlarged cavity sizes near the top of the layer with a typical 85 °C profile angle. This profile widening effect imposes a limit to the line proximity and aspect ratio achievable with positive resists.

Figure 3 illustrates the realization of copper lines, 10  $\mu\text{m}$  high, using STR1110 resist as a mold. The electrodeposition was carried out in a copper sulfate-sulfuric acid solution at 30 °C.

Positive resists are more sensitive to the plating solution than polyimides. They require a careful optimization of the prebake and postbake treatments



**Figure 2.** Positive photoresist mold, 17  $\mu\text{m}$  thick, used for delineating electrodeposited metal coils (the linewidth and pitch on the mask are 3.2 and 8  $\mu\text{m}$  respectively).



**Figure 3.** Electrodeposited copper lines after stripping the positive photoresist mold. The copper thickness is 10  $\mu\text{m}$ .

in order to avoid underplating, cracks or chemical interactions with the solution. The postbake treatment increases the resist adhesion and also partially destroys the photosensitive diazonaphthoquinone in non-exposed areas. Diazonaphthoquinone can react with the plating solution and release nitrogen, which may produce blisters in the layer. Excessive postbake temperatures will however induce profile distortion due to plastic flow in the photoresist. The resin may also become brittle and high thermomechanical stress can build up [20].

### 3. Electrodeposition

About 17 metals are commonly electroplated from aqueous solutions: Cr, Fe, Co, Ni, Cu, Zn, Ru, Rh, Pd, Ag, Cd, In, Sn, Ir, Pt, Au and Pb. Only a few of these have properties that make them useful in microstructure electrodeposition. Nickel, the most versatile metal in micromechanics, combines appropriate mechanical properties such as Young's modulus, yield strength and hardness with good corrosion resistance as well

as many interesting electroplating bath formulations. Copper and gold add to their intrinsic high electrical conductivities a particular ease of plating for copper and very good chemical resistance for gold. Other metals have not yet found wide applications in this field but the intrinsic properties of some of them might prove useful in specific applications. In addition to pure metals, alloy electrodeposition is also possible. More than one hundred alloys have been studied; however, only a few of these are commercially plated, such as FeNi, FeCo, NiP, CoNiP, CoW, AuNi, SnPb, SnCu, SnNi and CuZn. FeNi and FeCo have soft magnetic properties while NiP and CoNiP have hard magnetic properties. Alloys of gold are used for electrical contacts, alloys of tin, indium and lead as solder alloys.

Practical guidelines for metal and alloy electrodeposition can be found in the literature [21, 22].

'Electroless' or 'autocatalytic' plating is another industrial electrochemical process that has been applied to microstructure fabrication [23, 24]. The principle is the deposition of a metal on a surface from a solution containing simultaneously the metal salt and a reducing agent. Under appropriate conditions, the chemical reduction of the metal occurs only on catalytic surfaces; this implies of course that the metal itself is catalytic. Its distinctive advantages are the possibility of plating on insulators after an appropriate pretreatment, the absence of an external source of current and a practically perfect throwing power, i.e. a metal thickness independent of the surface topology. Nickel, cobalt, copper, palladium, gold and silver can be deposited in this way. Achievable maximum deposition rates are about 0.3  $\mu\text{m min}^{-1}$  for nickel and 0.1  $\mu\text{m min}^{-1}$  for copper [25]. Electroless deposition is an extremely useful technique, but with deposition rates more difficult to control and lower than in electrodeposition. It is not included in the following discussion since its use in microfabrication has been limited to specific cases.

Bath chemistry and electrodeposition reactions are quite complex but the control of the overall deposit thickness is simple. Electrodeposition at constant current  $I$  through a mask with an opened surface  $S$  will result in an average thickness  $e$  given by

$$e = RitM / SdnF$$

where  $t$  is the time,  $M$  is the atomic weight of the metal,  $n$  is the number of electrons exchanged,  $d$  is the density of the deposit,  $F$  is the Faraday constant (96500 C mole $^{-1}$ ) and  $R$  is the yield of the electrodeposition. Typical yields of 40% to 100% have been measured, competitive electrode reactions such as hydrogen codeposition being responsible for less than 100% yields. Current densities vary typically in the range of 1–100 mA cm $^{-2}$  and usual plating rates between 0.05 and 2  $\mu\text{m min}^{-1}$ .

Electrodeposition equipment is in principle simple. It consists of an adjustable constant-current source and a cell with a thermostat, preferably with controlled stirring and continuous filtration of the solution.

### 3.1. Electrodeposition requirements

A number of specific requirements have to be met for insuring a successful fabrication process. The photoresist material must be stable in the electrodeposition solution and provide a good adhesion to the substrate throughout the process. As a rule, acid plating solutions are much less aggressive than basic solutions, in particular towards positive photoresists, and higher solution temperatures increase the requirement for resist stability.

The electrical resistance of the seed layer must be low enough (typically  $0.5 \Omega$  per square) to provide a uniform current distribution. The seed layer must have a good adhesion to the substrate. It must be free of any organic residue and provide a good plating base to the electrodeposited metal. If the seed layer must be removed after plating (sacrificial layer), the etching process should not attack the plated metal. Sputtered or evaporated seed layers are usually composed of a thin adhesion/barrier and a conductive layer. Depending on the fabrication process various combinations are used such as Cr-Cu, Cr-Cu-Cr, Cr-Au, Cr-Ag, Ti, Ti-Au, Ti-Ni-Pd and TiW-Au.

Deposit thickness uniformity depends on the electrodeposition cell design, the solution composition and agitation, the current density and the size and uniformity of the patterns in the photoresist. Various analytical and finite-element methods have been developed to describe the influence of these parameters [33]. With a careful design of the layout and adequate plating conditions, thicknesses will be controlled routinely to  $\pm 10\%$  and in favourable cases to better than  $\pm 3\%$  [26].

Properties of the deposit such as morphology (grain size, surface roughness), electrical resistivity, mechanical behavior (hardness, tensile strength, internal stress) can vary greatly with the plating solution composition and electrodeposition conditions. The residual stresses play a very important role in micromechanical applications, especially when large thicknesses are involved. Stresses can induce deformations of the microstructures, delamination of the deposited layer and cracks in thin supporting membranes. They can be compressive or tensile from  $-50$  to  $+150 \text{ kg mm}^{-2}$  [22]. Some of these plating-dependent effects are described in the literature for FeNi alloy electrodeposition. FeNi has been extensively studied for its magnetic properties as well as its applications as a protective and decorative coating [27-29]. In the CSEM process, the FeNi alloy is electrodeposited at  $50^\circ\text{C}$  from a commercial bath with Ni (as sulfate and chloride), Fe (as sulfate), boric acid and proprietary stabilizer, brightener, stress reducing agent and wetting agent. The alloy composition is very dependent on the pH of the solution and current density as shown in figure 4. In addition, the pH of the solution strongly influences the internal stresses in the FeNi alloy (see figure 5). The composition of the alloy is controlled to  $\pm 3\%$  and the thickness uniformity to  $\pm 10\%$  with a plating rate of  $0.6 \mu\text{m min}^{-1}$ . The

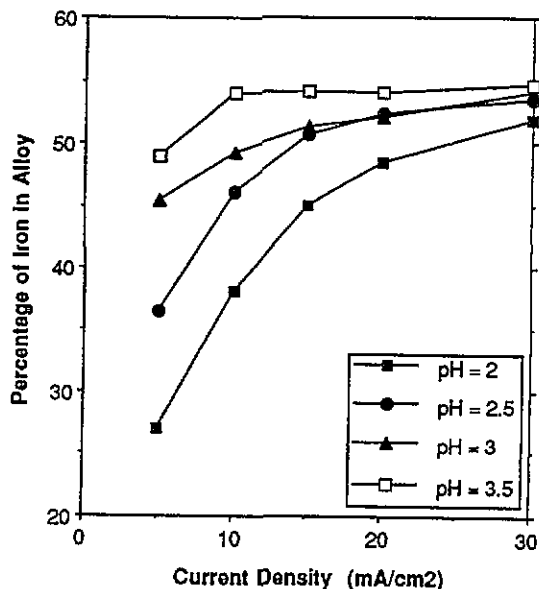


Figure 4. Dependence of the FeNi alloy composition on current density and pH of the solution.

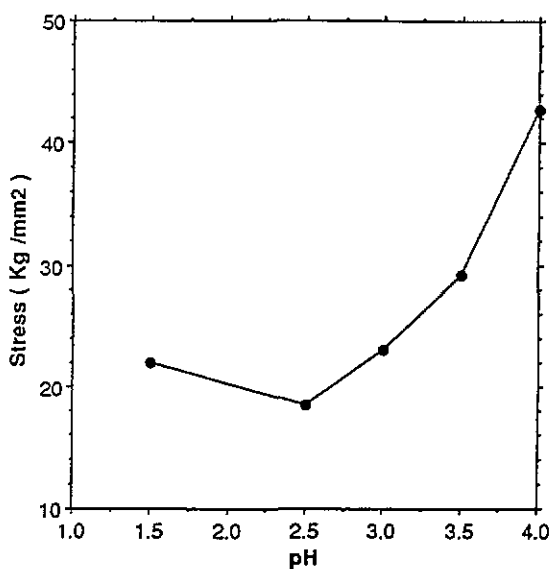


Figure 5. Dependence of the FeNi alloy stress on the pH of the solution.

resulting magnetization curve of this alloy is shown in figure 6. The saturation induction is  $1.45 \text{ T}$  and the coercive force is  $0.9 \text{ Oe}$ .

More elaborate 3D metal structures can be achieved by a multilevel process. Once the electroplated metal has filled the openings in the first photoresist layer, the seed layer deposition, photoresist coating and patterning steps are repeated and followed by electrodeposition of a second metal layer. The success of this operation greatly depends on the stability of the photoresist layers during the successive seed-layer deposition and electroplating steps.

Another way for realizing 3D metallic structures is the electroforming method. In this technique, electroplating is not stopped once the openings in the resist are filled but is continued up to thicknesses of the order of one tenth of a millimeter. Release of the deposit from the substrate results in a free-

microelectromagnet is composed of a flat 10-turn coil surrounded by a magnetic circuit consisting of a core extending through the silicon substrate and of a large backplate located under the coil. The magnetic circuit is made of a 50/50 FeNi alloy, a material chosen for its high saturation induction (1.5 T) and its low coercive force (0.9 Oe) (see figure 6 and [31]). The electrical circuit, which is designed for currents up to 1 A and low power consumption, has two metal levels. The first level, made of aluminium, is used for connecting the diodes, the second, made of gold, is dedicated to the coils and high-current interconnection lines. Gold was chosen for its low resistivity ( $2.5 \mu\Omega \text{ cm}$ ) and its ease of electrodeposition in thick layers.

Fabrication starts with standard microelectronic processes for the realization of the diodes and aluminium interconnects. The first metal level is covered by a silicon dioxide layer in which connecting vias are opened. A titanium-gold seed layer is sputtered on the front side and a  $4 \mu\text{m}$  thick positive photoresist is spun and patterned. Gold is electrodeposited through the resist mask from a commercial neutral gold cyanide solution at  $50^\circ\text{C}$  with a deposition rate of  $0.2 \mu\text{m min}^{-1}$ . After removal of the photoresist, the seed layer is etched, thus achieving the electrical insulation of the  $4 \mu\text{m}$  thick gold conductors. This process has proved to be particularly suited for defining the fine coil structures made of  $4 \mu\text{m}$  lines at a pitch of  $8 \mu\text{m}$  (see figure 8). The magnetic circuit is a 3D microstructure achieved in two silicon micromachining and three FeNi electrodeposition steps. The thin silicon membrane is obtained by anisotropically etching the wafer from the back. A seed layer is then evaporated and FeNi is selectively electrodeposited on the silicon membrane. Holes are anisotropically etched through the silicon membrane from the front side. Planarization of the front side is obtained by selectively filling the holes with electrodeposited FeNi, using the backplate as the electrical contact while keeping the back of the wafer insulated from the solution. Finally the FeNi cores are completed in the same way using a  $40 \mu\text{m}$  thick polyimide resist mold.

This process has been successfully applied to the fabrication of printing heads, as shown in figure 8, for a new generation of magnetographic printers.

#### 4.2. Micromachined capacitive microphone

The second example applies to the batch fabrication

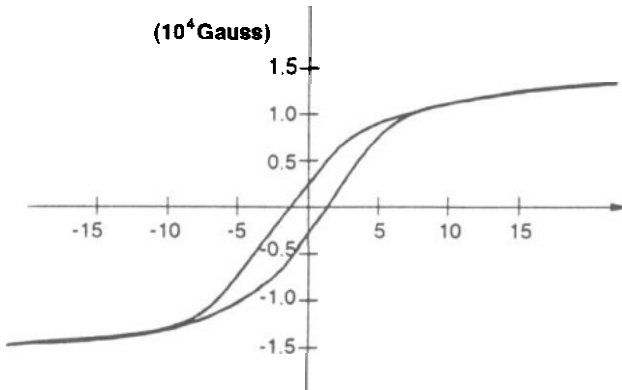
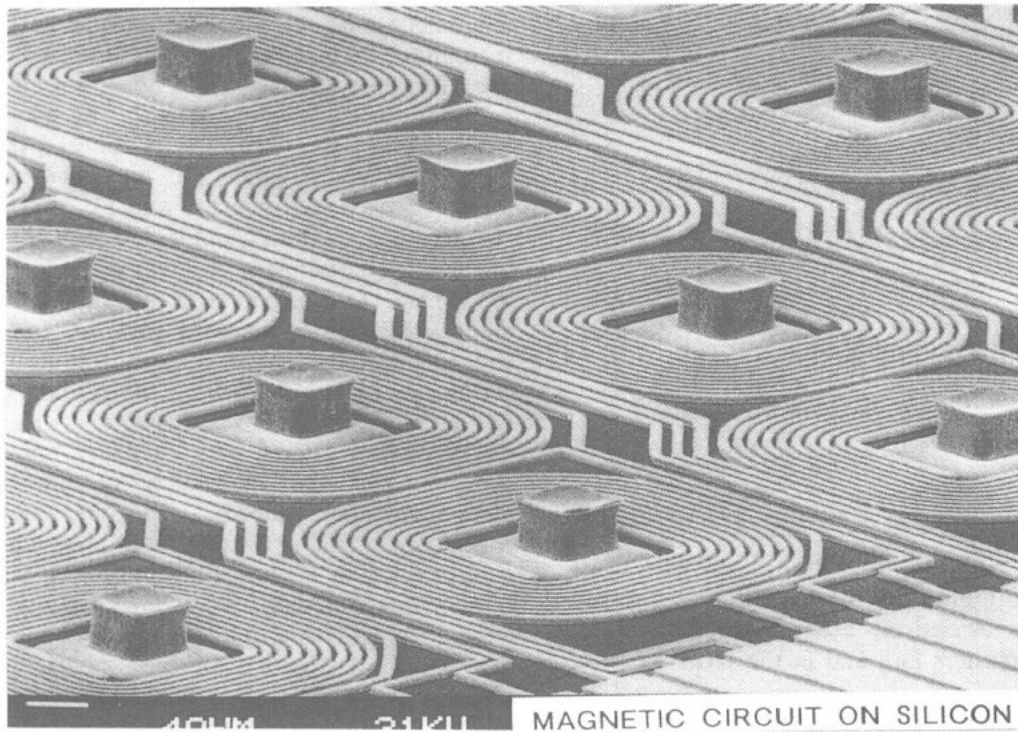


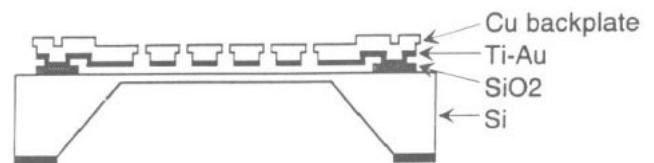
Figure 7. Schematic cross-section of an electromagnet and its addressing diode.



**Figure 8.** SEM view of the printing head made of 4  $\mu\text{m}$  linewidth gold coils at a pitch of 8  $\mu\text{m}$ , and of FeNi writing poles, 40  $\mu\text{m}$  high.

of a microphone. This microphone is composed of a pressure-sensitive diaphragm and a structured rigid backplate. These elements are the electrodes of a parallel-plate capacitor with a thin air gap in between, as shown in figure 9. The technology developed for implementing this structure uses a membrane of monocrystalline silicon for the diaphragm and selectively electrodeposited copper for the backplate. The electrodes are electrically insulated and mechanically separated by oxide spacers.

The fabrication process utilizes the following steps. The silicon wafer is thermally oxidized and the 3  $\mu\text{m}$  thick oxide is structured. A sacrificial negative resist is spun and patterned to uncover the oxide support areas. After evaporation of a titanium–gold seed layer on top of the structure, the gold layer is structured by means of a positive resist and a gold etch solution. The titanium provides the required adhesion to the oxide spacers, the gold to the copper backplate. A second 4  $\mu\text{m}$  thick negative photoresist is applied and patterned. This layer defines the plating mask for the electrodeposition of the backplate with its acoustic holes. Electrodeposition is performed in a sulfuric acid–copper sulfate bath at 40 °C, which results in a coarse grain and low-stress deposit. Up to 15  $\mu\text{m}$  thick copper layers have been electrodeposited to rigidify the microphone backplate. The overgrowth results in a mushroom structure and appropriate acoustic holes. After anisotropic silicon etching in potassium hydroxide, the wafers are diced and the two remaining photoresist layers with the titanium layer between them are stripped using wet as well as dry etching techniques.



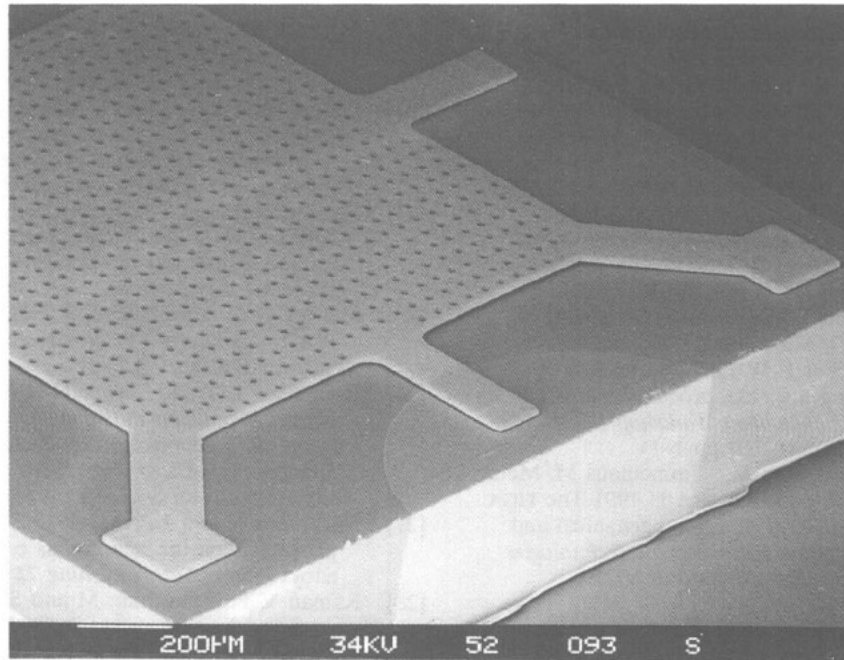
**Figure 9.** Schematic cross-section of the micromachined capacitive microphone.

Figure 10 shows an overall view of a finished microphone having a size of 2.4  $\times$  2.4 mm<sup>2</sup>. The measured prototype sensitivity is 1.4 mV Pa<sup>-1</sup> with an external bias voltage of 28 V. The frequency response is flat within  $\pm 3$  dB up to 14 kHz. These results are comparable to those obtained with other technologies [32]. The degrees of freedom offered by the microstructuring technique presented, in particular with respect to layer thickness and aspect ratio, should allow the improvement of device performance in the future. It also makes the integration of pre-amplifiers on the sensor chips possible.

## 5. Conclusions

Electrodeposition presents a number of interesting features. It is a mature and well established technique applying to many metals and metal alloys, which makes an accurate reproduction of mold openings possible with great conformity. Adequate seed layers are required but suitable choices are available.





**Figure 10.** SEM overall view of a finished microphone seen from the backplate side. The device size is  $2.4 \times 2.4 \text{ mm}^2$ .

Electrodeposition is a low-temperature process, which can be compatible with standard photoresist patterning techniques. The main restrictions arise from thickness and aspect ratio capabilities of presently available thick photoresists, their ability to withstand the plating solutions and the performance of associated photolithographic processes.

As demonstrated in the two applications presented in this paper, this technique is compatible with silicon surface and bulk micromachining as well as with the integration of associated electronics on the device. The utilization of sacrificial layers and that of multilevel metal layers further extend the application potential of this technique to more complex 3D microstructures.

### Acknowledgments

The authors want to gratefully acknowledge the support of Dr R Vuilleumier in editing this article. The authors also wish to thank Dr J-M Moret for his support and encouragement and Mr F Crevoisier for his assistance in carrying out the experimental work.

### References

- [1] Romankiw L T and Herman Jr D A (ed) 1990 Thin film inductive heads: from one turn to thirty one turns *Proc. Magnetic Materials, Processes and Devices (Hollywood, FL, 1989)* (Pennington, NJ: Electrochemical Society) pp 39–53
- [2] Löchel B, Maciossek A, Trube J and Huber H L 1990 Pulse plating of quarter micron gold patterns on silicon x-ray masks *Microelectron. Eng.* **11** 279–82
- [3] Guckel H, Christenson T R, Skrobis K J, Denton D D, Choi B, Lowell E G, Lee J W, Bajikar S S and Chapman T W 1990 Deep x-ray and UV lithographies for micromechanics *IEEE Solid-State Sensor and Actuator Workshop (Hilton Head, SC, 1990)* (New York: IEEE) pp 118–22
- [4] Takeda S, Ezawa H, Kuromaru A, Kawade K, Takagi Y and Suzuki Y 1989 Fine pitch TAB technology with straight side wall bump structure for LCD panel *IEEE Trans. Consumer Electron.* **CE-33** 343–51
- [5] Milosevic I, Perret A, Losert E and Schlenkrich P 1988 Polyimide enables high lead count TAB *Semicond. Int.* **10** 122–4
- [6] Schnackenberg U, Benecke W, Wälendusz V, Müller K P, Heuberger A and Lischke B 1989 Multi electron beam lithography: fabrication of a control unit *Microelectron. Eng.* **9** 205–8
- [7] Cardot F, Gobet J, Bogdanski M and Rudolf F 1993 Microfabrication of a high-density array of microelectromagnets with on-chip electronics *Digest Tech. Papers—Transducer 93 (Yokohama 1993)* pp 32–5
- [8] Ahn C H and Allen M G 1993 A fully integrated surface micromachined magnetic microactuator with a multilevel meander magnetic core *J. Microelectromech. Systems* **2** 15–22
- [9] Ahn C H, Kim Y J and Allen M G A planar variable reluctance magnetic micromotor with fully integrated stator and wrapped coils *Proc. IEEE Micro Electro Mechanical Systems Workshop (Fort Lauderdale, FL, 1993)* (New York: IEEE) pp 1–6
- [10] Fan L S, Lane L H, Robertson N, Crawforth L, Moser M A, Reiley T C and Imano W Batch-fabricated milli-actuators *Proc. IEEE Micro Electro Mechanical Systems Workshop (Fort Lauderdale, FL, 1993)* pp 179–82
- [11] Hirano T, Furuhashi T and Fujita H 1993 Dry released nickel micromotors and their friction characteristics *Digest Tech. Papers—Transducers 93 (Yokohama 1993)* pp 80–3
- [12] Frazier A B, O'Brien D P and Allen M G Two dimensional metallic microelectrode arrays for extracellular stimulation and recording of neurons



- Proc. IEEE Micro Electro Mechanical Systems Workshop (Fort Lauderdale, FL, 1993)* pp 195–200
- [13] Simon J, Engelmann G, Ehrmann O and Reichl H 1991 Plating of microstructures for sensors *Micro System Technologies 91* ed R Krahn and H Reichl (Berlin: VDE) pp 112–8
- [14] Kawahito S, Sasaki Y, Ishida M and Nakamura T 1993 A fluxgate magnetic sensor with micromachined solenoids and electroplated permalloy cores *Digest Tech. Papers—Transducers 93 (Yokohama, 1993)* pp 888–91
- [15] Ehrfeld W, Bley P, Götz F, Hagmann P, Maner A, Mohr J, Moser H O, Münchmeyer D, Schelb, Schmidt D and Becker E W 1987 Fabrication of microstructures using the LIGA process *Proc. IEEE Micro Robots and Teleoperators Workshop (Hyannis, MA, 1987)* (New York: IEEE) pp 1–11
- [16] Bley P, Göttert J, Harmening M, Himmelhaus M, Menz W, Mohr J, Müller C and Wallrabe U 1991 The LIGA process for the fabrication of micromechanical and microoptical components *Micro System Technologies 91* ed R Krahn and H Reichl (Berlin: VDE) pp 302–14
- [17] Allen M G 1993 Polyimide-based processes for the fabrication of thick electroplated microstructures *Digest Tech. Papers—Transducers 93 (Yokohama, Japan, 1993)* pp 60–5
- [18] Engelmann G, Ehrmann O, Simon J and Reichl H 1992 Fabrication of high depth-to-width aspect ratio microstructures *Proc. Micro Electro Mechanical Systems Workshop 92 (Travemünde, 1992)* (New York: IEEE) pp 93–8
- [19] Engelmann G, Ehrmann O, Simon J and Reichl H 1991 Development of a fine pitch bumping process *Micro System Technologies 91* ed R Krahn and H Reichl (Berlin: VDE) pp 435–40
- [20] Moreau W M 1988 *Semiconductor Lithography, Principle, Practice and Materials* (New York: Plenum) pp 545–66
- [21] Lowenheim F A 1978 *Electroplating* (New York: McGraw-Hill)
- [22] Safranek W H 1986 *The Properties of Electrodeposited Metals and Alloys* 2nd edn (Orlando, FL: American Electroplaters and Surface Finishers Society)
- [23] Furukawa S, Miyajima H, Mehregany M and Liu C C 1993 Electroless plating of metals for micromechanical structures *Digest Tech. Papers Transducers 93 (Yokohama, 1993)* pp 66–9
- [24] Parameswaran M, Xie D and Glavina P G 1993 Fabrication of nickel micromechanical structures using a simple low-temperature electroless plating process *J. Electrochem. Soc.* **140** L111–3
- [25] Mallory G O and Hajdu J B (ed) 1990 *Electroless Plating* (Orlando, FL: American Electroplaters and Surface Finishers Society)
- [26] Romankiw L T and Turner D R (ed) 1987 Electrodeposition in the electronic industry *Proc. Symp. on Electrodeposition Technology, Theory and Practice (San Diego, CA, 1986)* (Pennington, NJ: Electrochemical Society) pp 13–41
- [27] Nakamura N and Hayashi T 1985 Temperature and pH effects on the anomalous codeposition of Ni–Fe alloys *Plating Surf. Finishing* **72** pp 42–7
- [28] Raman V, Pushpavanam M and Sheno B A 1982 Some property data for nickel–iron alloy electrodeposits *Plating Surf. Finishing* **69** pp 132–6
- [29] Wagner U and Zilk A 1982 Selective microelectrodeposition of Ni–Fe patterns *IEEE Trans. Magn.* **MAG-18** 877–9
- [30] Legierse P E J 1987 Mastering technology and electroforming for optical disc systems *Trans. Inst. Met. Finishing* **65** 13–7
- [31] Josso E 1956 *Propriétés des Alliages Fer–Nickel à Haute Teneur en Nickel* (Paris: Centre d'Information du Nickel) pp 16–8
- [32] Bergqvist J, Rudolf F, Maisano J, Parodi F and Rossi M 1991 A silicon condenser microphone with a highly perforated backplate *Digest Tech. Papers Transducer 91 (San Francisco, 1991)* pp 266–9
- [33] Dukovic J O 1990 Computation of current distribution in electrodeposition, a review *IBM J. Res. Dev.* **34** 693–705